AIP Journal of Applied Physics

Annealing effect on nano-ZnO powder studied from positron lifetime and optical absorption spectroscopy

Sreetama Dutta, S. Chattopadhyay, D. Jana, A. Banerjee, S. Manik et al.

Citation: J. Appl. Phys. **100**, 114328 (2006); doi: 10.1063/1.2401311
View online: http://dx.doi.org/10.1063/1.2401311
View Table of Contents: http://jap.aip.org/resource/1/JAPIAU/v100/i11
Published by the AIP Publishing LLC.

Annealing effect on nano-ZnO powder studied from positron lifetime and optical absorption spectroscopy

Sreetama Dutta, S. Chattopadhyay,[a] and D. Jana[b]
Department of Physics, University of Calcutta, 92 Acharya Prafulla Chandra Road, Kolkata 700 009, India

A. Banerjee, S. Manik, and S. K. Pradhan
Department of Physics, University of Burdwan, Golapbag, Burdwan 713 104, India

Manas Sutradhar
Department of Chemistry, University of Calcutta, 92 Acharya Prafulla Chandra Road, Kolkata 700 009, India

A. Sarkar
Department of Physics, Bangabasi Morning College, 19 Rajkumar Chakraborty Sarani, Kolkata 700 009, India

(Received 12 June 2006; accepted 8 October 2006; published online 15 December 2006)

Mechanical milling and subsequent annealing in air at temperatures between 210 and 1200 °C have been carried out on high purity ZnO powder to study the defect generation and recovery in the material. Lowering of average grain size (from 76±1 to 22±0.5 nm) as a result of milling has been estimated from the broadening of x-ray lines. Substantial grain growth in the milled sample occurs above 425 °C annealing temperature. Positron annihilation lifetime (PAL) analysis of the samples shows a distinct decrease of the average lifetime of positrons very near the same temperature zone. As indicated from both x-ray diffraction (XRD) and PAL results, high temperature (>700 °C) annealed samples have a better crystallinity (or lower defect concentration) than even the nonmilled ZnO. In contrast, the measured optical band gap of the samples (from absorption spectroscopy) does not confirm lowering of defects with high temperature annealing. Thermally generated defects at oxygen sites cause significant modification of the optical absorption; however, they are not efficient traps for positrons. Different thermal stages of generation and recovery of cationic as well as anionic defects in granular ZnO are discussed in the light of XRD, PAL, and optical absorption studies.
 [DOI: 10.1063/1.2401311]

I. INTRODUCTION

Nanocrystalline materials, semiconductors in particular, are being widely investigated at present because of their interesting electronic and optical properties which may find applications in devices such as solar cells, light emitting diodes, ultraviolet (UV) lasers, fluorescent displays, etc.[1–4] Surface phenomena dominate nanomaterial properties over their respective bulk features due to high surface to volume ratio. Grain surfaces are defect rich, and engineering on these defects offer a scope to tune the useful material properties.[5] Here, we employ mechanical milling or ball milling technique to reduce the grain size of powder ZnO material. This technique is advantageous for large scale and cost effective production of nanocrystalline materials without any effect of chemical contamination.[6]

Recently, room temperature UV lasing has been reported in ZnO samples with grain size of a few tens of nanometers.[7,8] It has also been found that incorporation of low density defects in ZnO lattice sometimes helps to obtain improved crystalline quality through proper choice of annealing environment and temperature.[9] In this way, the extent of disorder and so also the characteristic emission from the material can effectively be controlled. A better understanding on the generation and recovery of defects in ZnO, particularly defects at grain surfaces, thus has immense potential to reach optimized annealing conditions. Suitable defect characterization technique such as positron annihilation lifetime spectroscopy has been proven to be helpful[3,10–13] in this regard. Usually, positrons injected inside a solid from a radioactive source (here ^{22}Na) get thermalized and annihilated with an electron. It is well known that positrons preferentially populate in the regions where electron density, compared to the bulk of the material, is lower (e.g., vacancy type defects, vacancy clusters, microvoids). For materials with nanometer scale grain size, positrons diffuse[14,15] to the surface region of the grains, which are rich in open volume defects. Hence the electron-positron annihilated γ rays bear the lifetime of positrons, which provides information regarding the nature and abundance of defects at the grain surface.[3,13,15,16] Simultaneous investigation of ultraviolate-visible (UV-vis) photon absorption by the sample elucidate, as will be detailed later, the defect dependent optical processes in such technologically important semiconductors.

II. EXPERIMENT AND DATA ANALYSIS

As-supplied polycrystalline ZnO powder (purity 99.9% from Sigma-Aldrich, Germany) samples have been ball

[a]Present address: Department of Physics, Taki Govt. College, Taki 743429, India.
[b]Author to whom correspondence should be addressed; FAX: 91-33-2351-9755; electronic mail: djphy@caluniv.ac.in

milled (ball:mass=35:1) by a Fritsch Pulverisette 5 planetary ball-mill grinder for 3 h and then annealed at ten different temperatures (between 210 and 1200 °C) for 4 h followed by slow cooling (30 °C/h) in air. Henceforth the milled but unannealed sample will be termed as nano-ZnO. X-ray diffraction (XRD) of all the samples have been recorded in a Philips PW 1710 automatic diffractometer with Cu $K\alpha$ radiation. The average grain size of the powdered samples has been determined by Scherer's formula:[17]

$$D_{hkl} = K\lambda/\beta \cos\theta,$$

where D_{hkl} is the average grain size, K is the shape factor (taken as 0.9), λ is the x-ray wavelength, β is the linewidth at half maximum intensity (here 101 peak of the ZnO spectrum fitted with a Gaussian), and θ is the Bragg angle. Standard method[17] to deduct the contribution of instrumental broadening in β has been taken into account.

Different sets of samples have been pressed into pellets (~1 mm thickness and 10 mm diameter) for positron annihilation lifetime (PAL) study. A 10 μCi ^{22}Na positron source (enclosed in thin Mylar foils) has been sandwiched between two identical plane-faced pellets. The PAL spectra have been measured with a fast-slow coincidence assembly[18] having 182±1 ps (Ref. 12) time resolution. Measured spectra have been analyzed by the computer program PATFIT-88 (Ref. 19) with necessary source corrections to evaluate the possible lifetime components τ_i and their corresponding intensities I_i. The two state trapping model[20] predicts a two-component fitting of the spectrum, the shorter one (τ_1) from free annihilation of positrons and the other (τ_2) from trapped positrons at defects. One can also construct, without assuming any model, the average positron lifetime $[\tau_{av}=(\tau_1 I_1 + \tau_2 I_2)/(I_1+I_2)]$, which represents the defective state of the sample as a whole.[19,21] It is to be noted that τ_{av} is free from errors, if any, arising from particular fitting procedure.

The electronic absorption spectra of the ZnO samples have been recorded on a Hitachi U-3501 spectrophotometer in the wavelength range of 300–1100 nm. The spectral absorption coefficient $\alpha(\lambda)$ has been evaluated[3,22] from the spectral extinction coefficient $k(\lambda)$ using the following expression:

$$\alpha(\lambda) = 4\pi k(\lambda)/\lambda,$$

where λ is the wavelength of the absorbed photon.

III. RESULTS AND DISCUSSION

The XRD spectra of the ZnO samples, ball milled and subsequently annealed at 600 and 1200 °C, have been shown in Fig. 1. Mechanical milling reduces the average grain size from 76±1 nm (as-supplied ZnO) to 22±0.5 nm (nano-ZnO). Annealing at elevated temperatures induces an agglomeration of grains in the sample, however, appreciable grain growth occurs only above 425 °C (Fig. 2). It is interesting to note that the average grain size of the samples annealed higher than 776±8 °C (as estimated from Fig. 2) becomes larger than that of the as-supplied or nonmilled material. Chen *et al.*[9] have reported similar observation in single crystalline ZnO, where initial amorphization by energetic Al^+ irradiation and subsequent heat treatment dramatically improve the crystalline quality and so also the band edge emission. Increase of average grain size, in our case, continues up to 1100 °C annealing temperature and reaches to 139±2 nm. Reduction of the grain size to ~15 nm in 1200 °C annealed sample is, probably, due to thermally generated defects at both Zn and O sites.[23]

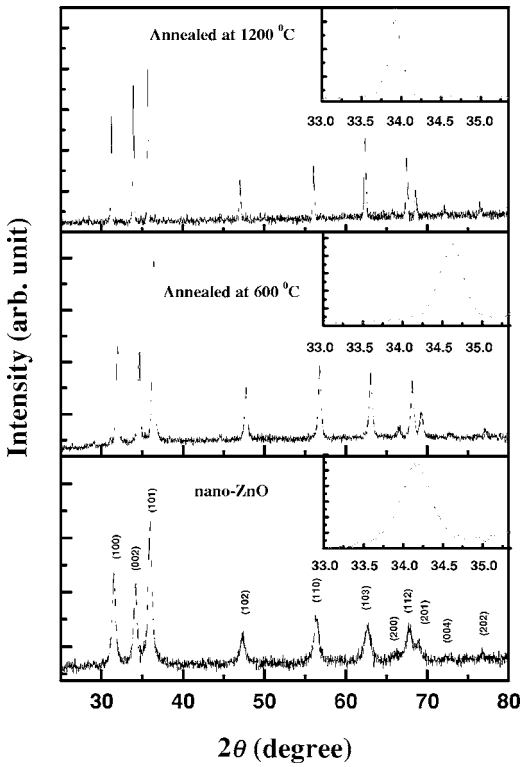

FIG. 1. X-ray diffraction patterns for the nano-ZnO and annealed ZnO samples. Insets show the corresponding full width at half maximum (FWHM) for (002) peak.

PAL analysis reveals a three-component lifetime fit, the third (τ_3) and the longest (~1400 ps with intensity 3%–4%) being due to the positron annihilation from positronium-

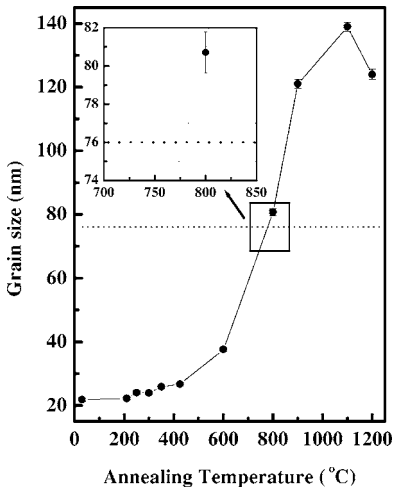

FIG. 2. Variation of grain size with annealing temperature. The annealing temperature of nano-ZnO sample has been taken as 30 °C (room temperature). The solid line is a guide to the eyes, and the dotted line is the reference line indicating the grain size for the nonmilled (as-supplied) sample.

TABLE I. Table showing the *c*-axis lattice parameter (from XRD), band tailing parameter, E_0 (from optical absorption), and part of the PAL parameters for the ZnO samples. For comparison the corresponding values of the as-supplied (nonmilled) material has been shown. The annealing temperature of nano-ZnO sample has been taken to be room temperature (RT) ~30 °C.

Sample	Annealing temperature (°C)	*c* axis (Å)	E_0 (meV)	τ_1 (ps)	I_1 (%)	I_2 (%)
As-supplied ZnO	RT	5.160	92	147±2	38.0±0.5	58.0±0.5
nano-ZnO	RT	5.242	316	173±2	32.3±0.2	64.5±0.2
	210	5.172	320	181±2	29.8±0.2	66.4±0.3
	250	5.168	300	214±2	47.0±0.2	49.4±0.2
	300	5.166	255	201±2	41.3±0.2	55.0±0.2
	350	5.182	201	184±2	36.4±0.2	60.2±0.3
	425	5.197	226	186±2	40.9±0.2	55.2±0.2
	600	5.177	214	159±2	31.6±0.2	64.1±0.3
	800	5.258	258	163±2	50.4±0.2	46.0±0.2
	900	5.264	386	151±2	57.9±0.3	38.3±0.2
	1100	5.272	523	151±2	59.7±0.3	35.8±0.2
	1200	5.279	676	153±2	61.5±0.3	34.2±0.2

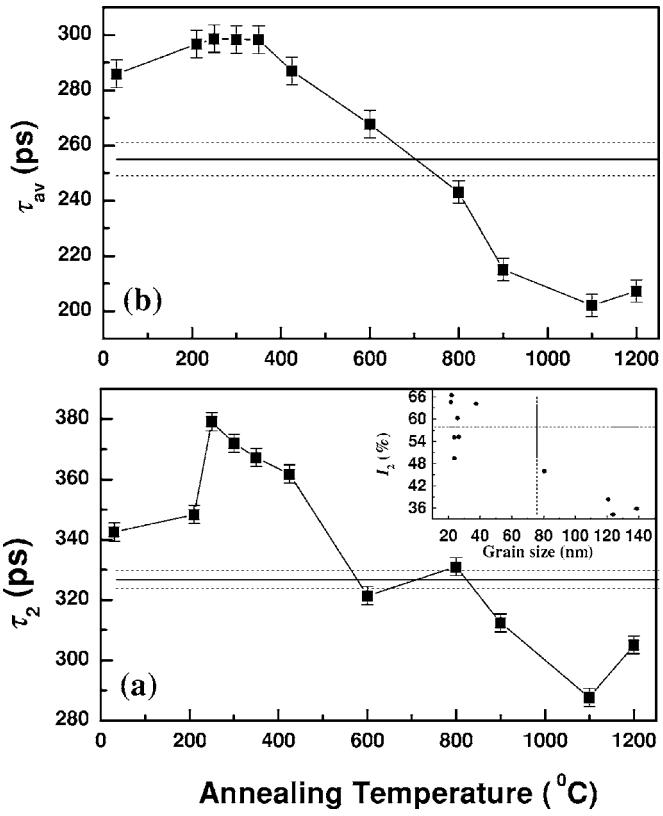

FIG. 3. Variation of (a) τ_2 (positron lifetime at defects) and (b) τ_{av} (average positron lifetime) with annealing temperature. The dotted lines are the reference lines corresponding to the error bars of the average positron lifetime and positron lifetime at defects (indicated by solid line) for nonmilled ZnO sample. The annealing temperature of nano-ZnO sample has been taken as 30 °C (room temperature). The inset of lower panel shows the variation of I_2 with grain size. The same parameters of the nonmilled ZnO are represented by the dashed lines in the inset.

like[21] atoms. Formation of positroniums generally occurs in the form of orthopositronium inside large voids in the material. Orthopositroniums subsequently decay as parapositronium by pickoff annihilation, giving rise to such a long lifetime ~1200–3000 ps. In polycrystalline samples there always exist void spaces where positronium formation is favorable.[12] To note, positronium formation in the material is a separate physical process not related to positron trapping at defects. τ_1 is generally attributed to the free annihilation of positrons.[21,24] However in disordered systems, smaller vacancies[9,16] (like monovacancies, etc.) or shallow positron traps (like oxygen vacancies[25] in ZnO) may be mixed with τ_1. In the present investigation, τ_1 from different ZnO samples show considerable variation with annealing temperature (Table I). τ_1, here, is indeed a weighted average of free and trapped positrons. But these sites are not major positron traps and their correlation with the material properties is not yet conclusive. The most important lifetime component is the second one (τ_2), which indicates qualitatively the nature and size of the vacancy[20] and its relative intensity (I_2) quantifies the abundance of that vacancy with respect to some standard of the same material. Here, τ_2 increases from 326±3 to 343±3 ps due to mechanical milling [Fig. 3(a)]. Enhanced vacancy clustering near the grain surfaces as a result of milling can be understood. While annealing the nano-ZnO material an increase of τ_2 with initial annealing up to ~300 °C has been found. This is similar to what we have observed for as-supplied ZnO (Ref. 12). Probably, the supply of small thermal energy helps intragrain zinc vacancies to migrate towards the grain surfaces, which are the universal sink of defects. In this way, small size Zn vacancies (monovacancies, etc.) assemble near the grain surfaces and τ_1 grows accordingly (Table I). Part of such vacancies agglomerate to form larger size vacancy clusters causing an increase of τ_2 also. Such a process can be understood as an intrinsic feature of granular ZnO systems that causes the increase of positron lifetime up to some annealing temperature ~300 °C. The variation of average lifetime (τ_{av}) with annealing temperature is more or less similar to that of τ_2 [Fig. 3(b)]. τ_{av} starts to decrease above the annealing temperature of 425 °C, interestingly, which is very close to the temperature from where the XRD spectrum shows a substantial grain growth. One should note here that positrons have a specific affinity towards cationic defect sites, which are generally negatively charged in these II-VI semiconductors.[10,24] So, the reduction of τ_2 as well as τ_{av} above 425 °C annealing represents a lowering of Zn vacancy defects at the grain boundaries, and consequently, grain growth occurs. Mobility of interstitial Zn defects above 425 °C may be the reason for Zn vacancy annihilation.[26] It can be estimated from Fig. 3(b) that above 700±50 °C annealing temperature the annealed sample becomes less defective compared to the nonmilled one. Similar conclusion has been reached while discussing the grain size variation of the annealed samples, and the related temperature zone also close to that has been estimated from the variation of grain size (776±8 °C). In view of the qualitative probing by two different techniques, such consistency is remarkable. Alternatively, our results altogether confirm the clustering of cationic vacancies at grain boundaries in ZnO nanocrystals. At the same time, it can also be concluded that majority of such cation vacancies, incor-

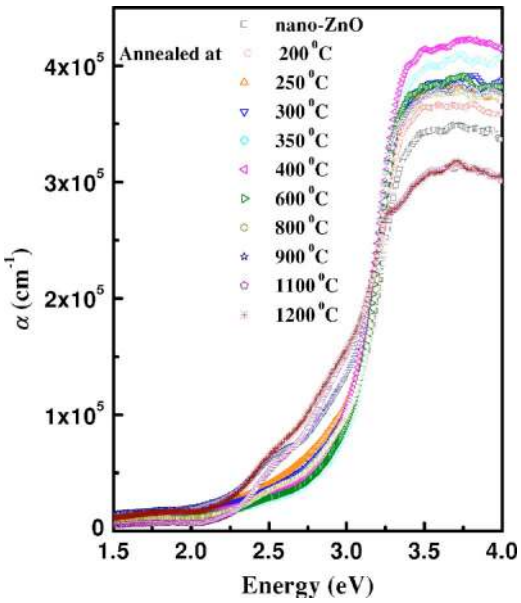

FIG. 4. (Color online) Absorption coefficients near the UV edge as a function of photon energy for the ZnO samples annealed at different temperatures.

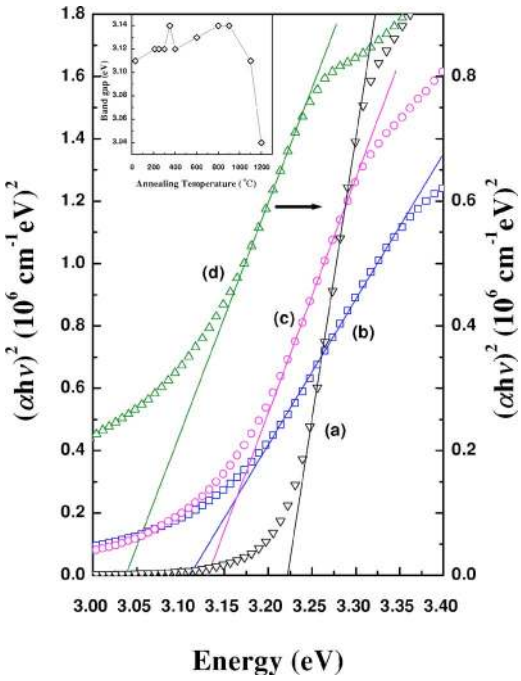

FIG. 5. (Color online) Plots of $(\alpha h\nu)^2$ vs photon energy for (a) as-supplied ZnO sample, (b) nano-ZnO sample, (c) sample annealed at 600 °C, and (d) sample annealed at 1200 °C. The inset shows the variation of band gap with annealing temperature.

porated artificially either by particle irradiation[9,26] or by mechanical milling (present case), in ZnO gets recovered in between 700 and 800 °C. Compared to 1100 °C annealed sample, the defect lifetime (τ_2) has been found to be increased for 1200 °C annealed sample. Chen *et al.*[27] have also found an increase of positron lifetime above 1000 °C in single crystal ZnO. Such increase of positron lifetime is due to the enhancement of cationic vacancy sites. A reflection of the large number of thermal vacancy generation, anionic as well as cationic, is also evident from the lower grain size of the 1200 °C annealed sample with respect to the 1100 °C annealed one (Fig. 2). Here we should briefly mention the variation of I_2 (i.e., the relative intensity of τ_2) due to annealing. I_2 is related (but not proportional) to the abundance of defects in the material that gives rise to a positron lifetime of τ_2. It has been mentioned earlier that in materials with few tens of nanometer grain size, most of the defects reside near the grain surfaces where positrons annihilate. With annealing induced grain growth, the ratio of surface to bulk region decreases in the material. Hence, in our nano-ZnO system also, we should expect a correlation[15] between I_2 and the grain size, which has been plotted in the inset of Fig. 3(a). A general trend of lowering I_2 with increasing grain size can be identified although below 38 nm there exists some subtle features which are not understood at this stage. Below a certain grain size, other type of defects such as dislocations, microstrain, etc., which are very much likely in such mechanically milled nanosystems, may partly contribute to I_2.

The photon energy dependence of the optical absorption coefficients of the milled and annealed samples has been shown in Fig. 4. The optical band gap (E_g) of the samples have been estimated from the well known expression[28] for direct transition

$$\alpha E = A(E - E_g)^{1/2},$$

where $E(=hc/\lambda)$ is the photon energy and A is a constant. Standard extrapolation of absorption onset[28] to $\alpha E=0$ (where $E=E_g$) has been figured for selected samples (Fig. 5) along with the modification of band gap due to annealing (inset of Fig. 5). The nano-ZnO has a lower optical band gap (3.11 eV) compared to the nonmilled or as-supplied one (3.22 eV), which is probably due to its more granular nature.[29] Annealing above 900 °C temperature induces a redshift in the band gap, which is consistent with earlier reports.[24,30,31] Possible reason may be the increase of oxygen vacancy related disorder for annealing at high temperature. Enhanced oxygen vacancy in ZnO lattice is also evident from the expansion[12,32] of c-axis lattice parameter above 800 °C annealing, as shown in Table I.

We further plotted for all the samples $\ln(\alpha)$ vs E graph (Fig. 6) just below the band edge ($E<E_g$) to understand the band tailing effect due to enhancement/reduction of defects with annealing. According to the theory,[28] $\alpha(E)$ should follow

$$\alpha(E) = \alpha_0 \exp(E/E_0),$$

where α_0 is a constant and E_0 is an empirical parameter. E_0 has been estimated from the reciprocal of the slope by fitting the linear part of the respective $\ln(\alpha)$ vs E curves. Any defect or disorder in the lattice gives rise to localized states within the band gap (band tailing), and E_0 describes the width of such localized states.[29] Enhancement of E_0 indicates the increase of disorder in the system. It has been found that the 350 °C annealed sample shows the lowest E_0 value (Table I). Interestingly, we have also observed a reduced E_0 due to annealing of as-supplied ZnO near the same temperature zone.[33] However, the degree of disorder as reflected from the value of E_0 is higher for nano-ZnO along with its annealed counterparts than the as-supplied material. E_0 starts increasing steeply with the increase of annealing temperature from

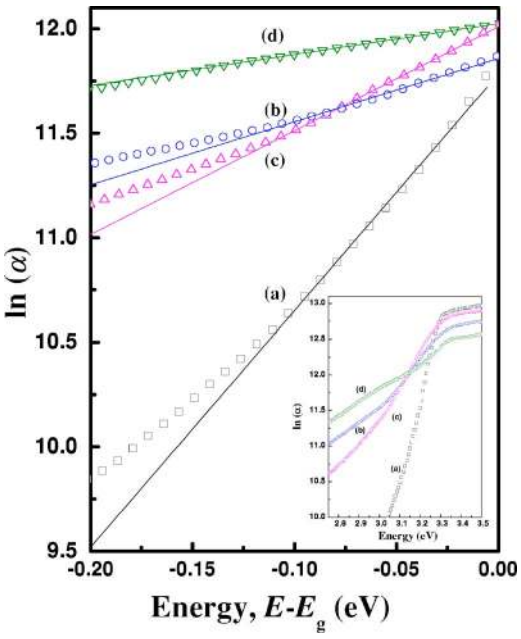

FIG. 6. (Color online) Plots of $\ln(\alpha)$ vs photon energy for (a) as supplied nonmilled ZnO sample, (b) nano-ZnO sample, (c) sample annealed at 350 °C, and (d) sample annealed at 1200 °C to show the linear variation of the respective curves. The inset shows the same curves in a broader region.

800 °C. In contrast, the PAL investigation reveals (discussed earlier) a considerable lowering of defects due to annealing above 700±50 °C. This is due to the fact that the relative trapping probability of positrons at an oxygen vacancy is much weaker compared to that of a zinc vacancy. Within 700–800 °C most of the zinc vacancies are recovered, but at this stage, thermally generated oxygen vacancies become dominant defects in the ZnO lattice. Oxygen vacancy and its related disorder create localized defect states within the band gap, resulting in an increase of the band tailing parameter E_0 and a redshift of the band gap.

IV. CONCLUSION

We have studied the effect of mechanical milling and subsequent annealing in air at temperatures between 210 and 1200 °C on high purity ZnO by XRD, PAL, and optical absorption spectroscopy. The grain size has been reduced to 22±0.5 nm (nano-ZnO) from 76±1 nm (as-supplied ZnO) due to milling. The XRD analysis reveals a substantial grain growth in nano-ZnO above 425 °C temperature. Distinct decrease of the average lifetime of positrons also starts from the same temperature. This indicates a lowering of defect concentration, mostly cationic, due to annealing above 425 °C. Such a reduction of defects continues up to 1100 °C annealing, and a little above 700 °C the sample becomes less defective, even better than the as-supplied ZnO. However, the band tailing parameter (E_0), which has contributions from all possible disorders, does not reflect a lowering of defects for high temperature annealing (>700 °C). Enhanced oxygen vacancy concentration is responsible for such an increase of E_0. These oxygen vacancies are less sensitive to positron spectroscopic measurements. Only the increase or decrease of the zinc vacancies is reflected in the PAL results. The annealing induced grain growth occurs due to the recovery of such zinc vacancies, the majority of which reside near the grain surfaces. PAL results, thus, bear a qualitative similarity with the findings from XRD analysis. Oxygen vacancy related disorder (>800 °C) mainly contributes to the modification of UV-vis absorption spectrum, and thus positron lifetime and optical absorption spectroscopy provide different scenario regarding the defective state of the material.

ACKNOWLEDGMENTS

The authors are grateful to FIST-DST for providing financial assistance. One of the authors (M.S.) gratefully acknowledges CSIR, Government of India, for providing financial assistance. Two of the authors (D.J. and A.S.) acknowledge University Grants Commission, Government of India, for financial help in a minor research project (PSW-029/05-06). Authors are thankful to Professor G. N. Mukherjee, Department of Chemistry, University of Calcutta, for assistance in acquiring optical data of the samples.

[1] I. Shalish, H. Temkin, and V. Narayanamurti, Phys. Rev. B **69**, 245401 (2004).
[2] X. T. Zhou, P.-S. G. Kim, T. K. Sham, and S. T. Lee, J. Appl. Phys. **98**, 024312 (2005).
[3] M. Chakraborty, S. Dutta, S. Chattopadhyay, A. Sarkar, D. Sanyal, and A. Chakrabortyi, Nanotechnology **15**, 1792 (2004).
[4] M. Bredol and H. Althues, Solid State Phenom. **99–100**, 19 (2004).
[5] Y. S. Wang, P. J. Thomas, and P. O'Brien, J. Phys. Chem. B **110**, 4099 (2006).
[6] A. Urbieta, P. Fernández, and J. Piqueras, J. Appl. Phys. **96**, 2210 (2004).
[7] G. Tobin, E. McGlynn, M. O. Henry, J. P. Mosnier, J. G. Lunney, D. O'Mahony, and E. dePosada, Physica B **340–342**, 245 (2003).
[8] U. Özgür *et al.*, J. Appl. Phys. **98**, 041301 (2005).
[9] Z. Q. Chen, M. Maekawa, S. Yamamoto, A. Kawasuso, X. L. Yuan, T. Sekiguchi, R. Suzuki, and T. Ohdaira, Phys. Rev. B **69**, 035210 (2004).
[10] R. Krause-Rehberg and H. S. Leipner, *Positron Annihilation in Semiconductors* (Springer, Berlin, 1999), Chap. 3, p. 61.
[11] F. Tuomisto, V. Ranki, K. Saarinen, and D. C. Look, Phys. Rev. Lett. **91**, 205502 (2003).
[12] S. Dutta, M. Chakrabarti, S. Chattopadhyay, D. Sanyal, A. Sarkar, and D. Jana, J. Appl. Phys. **98**, 053513 (2005).
[13] M. Chakraborti, D. Bhowmick, A. Sarkar, S. Chattopadhayay, S. DeChoudhuri, D. Sanyal, and A. Chakraborti, J. Mater. Sci. **40**, 5265 (2005).
[14] A. Dupasquier and A. Somoza, Mater. Sci. Forum **175–178**, 35 (1995).
[15] V. Thakur, S. B. Shrivastava, and M. K. Rathore, Nanotechnology **15**, 467 (2004).
[16] P. M. G. Nambissan, C. Upadhyay, and H. C. Verma, J. Appl. Phys. **93**, 6320 (2003).
[17] B. D. Cullity, *Elements of X-ray Diffraction* (Addison-Wesley, Philippines, 1978), Chap. 9, p. 284.
[18] A. Banerjee, A. Sarkar, D. Sanyal, P. Chatterjee, D. Banerjee, and B. K. Chaudhuri, Solid State Commun. **125**, 65 (2003).
[19] P. Kirkegaard, N. J. Pedersen, and M. Eldrup, Riso National Lab Report No. Riso-M-2740, 1989.
[20] P. Hautojarvi and C. Corbel, in *Positron Spectroscopy in Solids*, edited A. Dupasquier and A. P. Millis, Jr. (IOS, Amsterdam, 1995), p. 491.
[21] D. Sanyal, D. Banerjee, and U. De, Phys. Rev. B **58**, 15226 (1998).
[22] A. A. Dakhel and F. Z. Henari, Cryst. Res. Technol. **38**, 979 (2003).
[23] Z. Z. Zhi, Y. C. Liu, B. S. Li, X. T. Zhang, D. Z. Shen, and X. W. Fan, J. Phys. D **36**, 719 (2003).
[24] R. M. de la Cruz, R. Pareja, R. Gonzalez, L. A. Boatner, and Y. Chen, Phys. Rev. B **45**, 6581 (1992).
[25] F. Tuomisto, K. Saarinen, D. C. Look, and G. C. Farlow, Phys. Rev. B **72**, 085206 (2005).
[26] Z. Q. Chen, M. Maekawa, A. Kawasuso, S. Sakai, and H. Naramoto, Physica B **376–377**, 722 (2006).
[27] Z. Q. Chen, S. Yamamoto, M. Maekawa, A. Kawasuso, X. L. Yuan, and T. Sekiguchi, J. Appl. Phys. **94**, 4807 (2003).

[28]J. Pancove, *Optical Processes in Semiconductors* (Prentice-Hall, Englewood Cliffs, NJ, 1979).
[29]V. Srikant and D. R. Clarke, J. Appl. Phys. **81**, 6357 (1997).
[30]N. R. Aghamalyan, I. A. Gambaryan, E. Kh. Goulanian, R. K. Hovsepyan, R. B. Kostanyan, S. I. Petrosyan, E. S. Vardanyan, and A. F. Aerrouk, Semicond. Sci. Technol. **18**, 525 (2003).
[31]R. Hong, J. Huang, H. He, Z. Fan, and J. Shao, Appl. Surf. Sci. **242**, 346 (2005).
[32]H. Kim, A. Piqué, J. S. Horwitz, H. Murata, Z. H. Kafafi, C. M. Gilmore, and D. B. Chrisey, Thin Solid Films **377–378**, 798 (2000).
[33]S. Dutta, S. Chattopadhyay, A. Sarkar, M. Sutradhar, and D. Jana (unpublished).